Seismic Resistance of RC Corner Eccentric Beam Column Sub-assemblages

Sabry Fayed [a]*, Ahmed G. Asran [b], Hassan H. EL-Esnawi [b], Ahmed Badr el-din [c]

a Associate Professor, Civil Engineering Department, Faculty of Engineering, Kafrelshiekh University, Egypt
b Professor of Concrete Structures, Faculty of Engineering, Azhar University, Egypt
c Civil Engineering Department, Higher Institute of Engineering and Technology, Kafr El sheikh, Egypt
* Corresponding Author Email Addresses: sabry_fayed@eng.kfs.edu.eg, sabrielmorsi@yahoo.com

Abstract: **An experimental investigation studied performance of Scorner beam-column connection (BCC) under cyclic loading. Each BCC consisted of upper, lower column and two beams; one of them was free end (A) while the other was fixed end (B). The cyclic loading was applied on the end of beam (A) while the beam (B) was unloaded and subjected to torsion stresses due to fixation. Two variables were investigated. The first is the eccentricity of the beam about column edge while the second is the effect of stirrup joint configuration on BCC under cyclic loading. All BCCs were tested under reversible fourteen cycles. The vertical displacement at the free end of the beam (A), horizontal sway at mid height of the column, crack and ultimate loads were observed in details at each cycle. The findings noticed that the increase of stirrup length in the connection decreased the deflection at the same level of the load. The ultimate load of specimen, which was shifted by 25mm, was less than the ultimate load of specimen, without shift, by 24%.When the joint stirrup was extended outside the column core by 50 mm in specimen Sp2, the capacity of the connection increased.**

Keywords— **RC; beam-column joint; experimental work; deflection; eccentricity; stirrups.**

1. INTRODUCTION

Beam column connections (BCC) are critical structural features in concrete constructions. This is owing to the difficulties of its construction and the complexity of its design. The BCC was the primary cause of collapse in some earthquake-damaged structures. Researchers have identified four types of failures that can occur in BCC. Shear failure in the joint, sliding of the beam main reinforcement bars, yielding of the beam main reinforcement (beam hinging), and yielding of the column longitudinal bars are the many types of failure (column hinging). Several moment-resisting frame constructions failed due to shear failure of BCC during recent earthquakes.

During earthquakes, structures intended for typical loads are frequently damaged or collapse. Recent earthquake measurements suggest that many RC constructions have failed in the brittle behaviour of beam-column joints due to a lack of seismic features in the joint panel. Beam-column joints are considered a complicated and demanding assignment for structural engineers, and careful design of joints in RC frame structures is critical to the structure's safety. Although the size of the junction is determined by the size of the frame parts, joints must withstand a set of loads passed from beams and columns.

Because the stresses concentrate close to one side of the column core, the behaviour of eccentric RC BCC is critical. The stresses transferred outside the column when the loaded beam is supported by another beam and the main steel of the loaded beam is extruded out of the column core. The effect of eccentric beams on joints, according to ACI 352-R02, is an issue that needs more investigation. When the beam centerline does not pass through the column centroid, the ACI guidelines can be used to the link, but only if all beam rebars are fixed in or pass through the column core. Because of a lack of research data on the anchoring of such beam bars in Type 2 connections under significant load reversals, eccentric connections with beam bars that pass beyond the column core are precluded. ACI defines Type 2 connections as those that are susceptible to earthquake loads. The behaviour of an eccentric joint with a beam rebar outside of the column was investigated in this work.

Yasuaki and Osamu [1] investigated the effect of eccentricity on the shear strength of reinforced concrete interior beam-column joints experimentally. The results demonstrate that as the eccentricity grew, so did the joint shear strength. Akanshu et al. [2] studied the strength and ductility of RC BCC. The minimal value of the peak horizontal joint shear stress sustained by internal joints was determined to be $1.33\sqrt{f_c}$. Hideo et al. [3] gathered 332 test data regarding the interior BCCs. They investigate a variety of characteristics that influence the shear strength of the interior BCCs. It was discovered that the concrete compressive strength had the greatest effect on the joint shear strength while the column axial force ratio and joint shear reinforcement ratio had little influence. Additionally, key criteria for determining the shear strength of BCCs without transverse reinforcement were provided by Sangjoon [4]. It was discovered that the shear strength of unreinforced external joints decreases as the joint aspect ratio increases. Jung [5] provided a technique for predicting the deformability of RC joints failing under shear once plastic hinges form at both ends of neighboring beams. [6] examined ten half-scale reinforced concrete beam-column joint sub-assemblages to failure using statically cyclic loading imitating earthquake loading to collect essential data such as stress in bars after yielding and joint deformation. It was discovered that the tale shear capacity of the specimen with transverse beams, which had extensive joint damage, could be enhanced.

Leslie [7] examined four exterior reinforced concrete beam-column sub-assemblages. Standard hook and the continuous U-bar detail were both evaluated as beam bar anchorage methods. The U-bar detail has a significant benefit in that it minimizes the complexity of reinforcing in the joint zone, allowing for quicker concrete application and compaction. Many studies [8–10] conducted experiments to assess the seismic performance of BCCs. Prior research looked

into deflection, ductility, strength, energy dissipation response, reinforcement detailed requirements, stiffness, and drift reversals. Many scholars [11-16] have carried out combined experimental and numerical investigations on the performance of BCCs. [17] described a numerical evaluation of the seismic behaviour of shear deficient BCC. Fayed et al. [18] investigated the behaviour of 3D constructions that included BCCs. The behaviour of structural components was examined in studies [19-37].

According to the American code [38], beams with major bars going through the column core should be investigated for eccentricity. This idea was considered in the current investigation. An RC corner eccentric beam-column joint's cyclic behaviour was illustrated. Furthermore, there was a research gap in the behaviour of RC BCC in the situation of two beams; in plane and out of plane, therefore the current study evaluated the performance of RC corner eccentric BCC exposed to cyclic load experimentally.

2. OBJECTIVES

The primary purpose of this research is to look at an experimental work done on a reinforced concrete beam column connection under cyclic loading. The following are the connected objectives: I) To investigate the behaviour of reinforced concrete beam column connections under cyclic loading; ii) To investigate the effect of beam eccentricity about the column edge; and iii) To investigate the effect of stirrup joint configuration on reinforced concrete beam column connections under cyclic loading.

3. EXPERIMENTAL PROGRAM

A. Materials

Concrete is a building material made of Portland cement and water, as well as sand and crushed stone. Table 1 provides the weighted components of the planned concrete mix for one cubic metre.

The concrete mixes were prepared to have a mean cube crushing strength of 35MPa after 28 days. To quantify the precise concrete compressive strength, 3 standard concrete cubes of size 150x150x150mm and three standard cylinders (150mm in diameter and 300mm in height) were cast for each specimen. To determine the tensile strength of the proposed concrete mix, two small plain concrete simple beams (105x108x360 mm) were casted for each specimen. Figure 1 shows the details of the sample. Moreover, splitting test was conducted using standard cylindrical specimens with diameter of 150mm and height of 300mm to determine the concrete tensile strength.

Table 1. Components of the planned concrete

Material	Cement	Fine aggregates	Coarse aggregates	Water	Admixture (super plasticizer)
Weight (kg)/m^3	350	637	1295	175	3.5 liters

Ordinary Portland cement with grade of 42.5 MPa was used in the concrete mix. The chemical and physical characteristics of the used cement satisfy the Egyptian Standard Specification No 2421-1993 [39].Fine, siliceous graded sand, free of chemicals, ashes, organic material sand impurities was used in the concrete mix. The utilized sand has a unit weight of 1700 kg/m^3. Dolomite, which has been quarried, crushed, and graded, is utilized as a coarse aggregate in the suggested concrete mix. Crushed dolomite had a maximum size of 15 mm and a unit weight of 1600 kg/m^3. Super plasticizer (Sikament163M) was utilized to provide an appropriate degree of workability in new concrete. The technical properties of Sikament163Mare listed in Table 2.
There were 2 kinds of steel reinforcing employed. The primary longitudinal reinforcement was made of high tensile steel (H.T.S) with a diameter of 12 mm and a nominal yield stress of 410 MPa. As transversal reinforcement, normal mild steel with a diameter of 6mm and a nominal yield stress of 250 MPa was utilized.

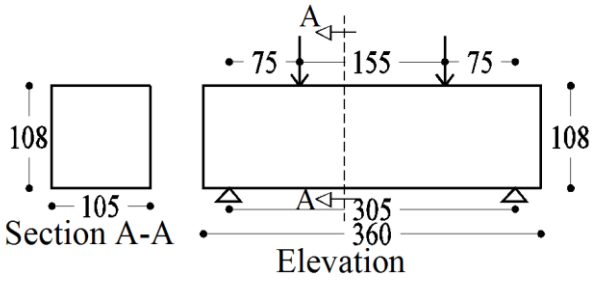

Figure 1. Details of the sample used in tensile flexural test

Table 2. Technical characteristics of Sikament163M

Appearance	Color	Specific gravity	Type	Application Dosage
Viscous liquid	Brown	1.2 Kg/later.	Polymer type dispersion	1ltr/100Kg of cement weight

B. Fabrication of specimens

Three modeled RCBCC specimens were used in the experiment. The current study took into account a corner beam-column coupling, as depicted in Figure 2. It was made up of a half-scale column linked on the top and bottom of the joint and a portion of the beam up to half the span, which corresponded to the sites of contra-flexure in the beam and column under lateral stresses. A typical full-scale residential structure with a floor to floor height (hc) of 3.9 m and an actual span of 3.6 m was evaluated. For the unloaded beam, the effective span was 4.5 m. The structural plan showed in Figure 3illustrates the dimensions of residential building considered in this research. For testing purposes, the connection was reduced to 1/3 its original size. For the isolation of a single unit of beam-column connections, symmetric boundary conditions were maintained at both ends of the column. Each specimen in the current study was made up of a column and two perpendicular beams. The first beam was loaded with reversible cyclic loads, whereas the second was not, hence it was referred to as the unloaded beam.

The Egyptian code (2007) [40] was employed in the specimen design. The size and reinforcing details are the same for all examples. Figure 4 depicts typical concrete dimensions for specimens, which are detailed in Tables 3 and 4. The column has a 100x200 mm cross section and a total height of 1300 mm. The column was joined to two beams 100 mm wide and 200 mm deep. The longitudinal direction of the column was reinforced by 4Ø12. Except for the junction panel, the transverse stirrups were 12 Ø 6/m.

The joint panel's shear reinforcement was a changeable parameter. The top and bottom primary longitudinal bars for loaded beam (A) were 2 Ø 12 in longitudinal direction, whereas 10 Ø 6/m were employed as vertical stirrups. The integrated length of the loaded beam's lower and upper main steel was 245 mm. The longitudinal main rebars was 2 Ø 12mm as top and bottom reinforcement for the unloaded beam (B). Furthermore, 10.6 Ø 6/m were utilized as stirrups.μ is volume ratio of stirrups and it was listed in Table 4 for all tested specimens.

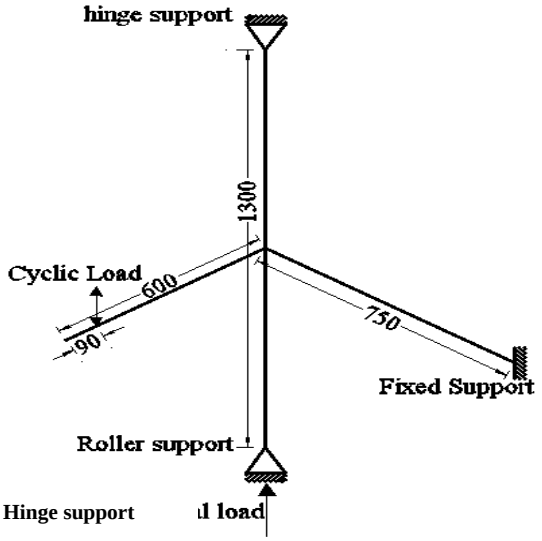

Figure 2 Corner isolated beam-column joint of all specimen

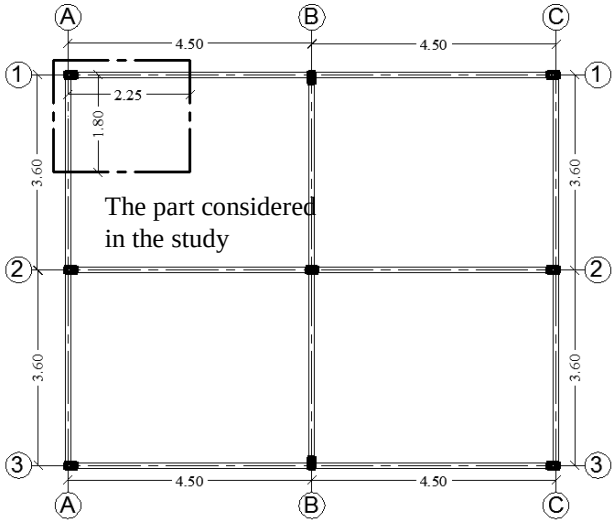

Figure 3. The dimensions of residential building that considered in the study.

In this study, μ was taken equal the ratio between stirrup volume of the joint and concrete volume of the joint (μ = V_s/V_c). Where $V_c = b_{eff} * h_c$ and b_{eff} defined as average between column width and beam width. Figure 5 depicts the reinforcing details for the tested specimens. Figure 6 depicts the joint reinforcement details for the tested specimen Sp2.

A strong form work from strengthened wood was used as a mold to cast in the specimens. A clear cover of 10 mm for all reinforcements was considered, see in Figure 7. After placing the steel form in forms, the casting process was divided into two main steps; the first is casting the column and the unloaded beam. The second step is fixing and casting the loaded beam.

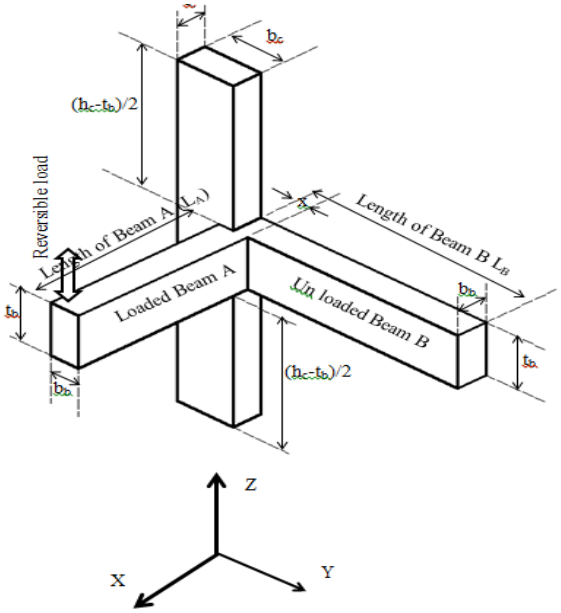

Figure 4. The typical concrete dimensions for specimens.

Table 3 Details of similar parameters

specimen	Beam A				Beam B				column				
	dimension		reinforcement		dimension		reinforcement		dimension			reinforcement	
	Cross sec.mm	Length mm	equal lower bars	stirrups	Cross sec.mm	Length mm	Top and bottom bars	stirrups	$b_c$mm	$t_b$mm	$h_c$mm	Longithdinal bars	stirrups
All specimens	100x200	600	2 D 12 mm	D 6 @ 100 mm	100x200	750	2 D 12 mm	D 6 @ 94.3 mm	200	100	1300	4 D 12 mm	D 6 @ 84 mm

Table 4 Details of different parameters of the tested specimens

specimen	Shear reinforcement of the Joint			(x) Shifting distance of the loaded beam (A) from column edge (mm)	Distance x/b_b
	Amount	Area (mm^2)	Volume ratio of stirrups (μ %)		
Sp	1 Ø 6	80x180	0.489	0	0 %
Sp	1 Ø 6	80x180	0.489	25	25%
Sp	1 Ø 6	80x240	0.489	50	50%

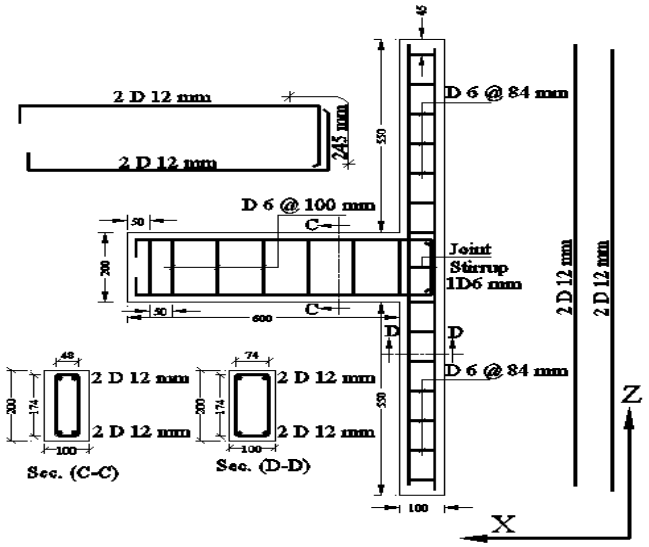

(a) Reinforcement configurations for the loaded beam A

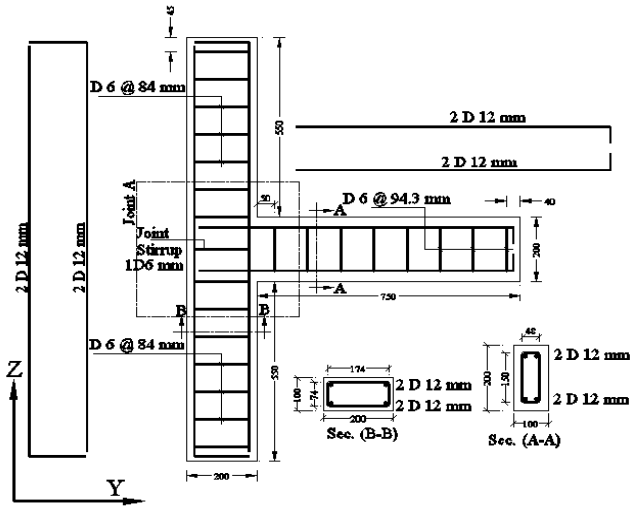

(b) Reinforcement configurations for unloaded beam B

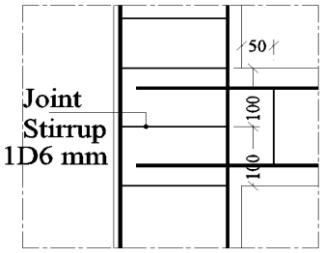

(c) Details of joint

Figure 5 Reinforcement configurations of the tested specimens Sp0 , Sp1

C. Mechanical properties of concrete and steel

Samples of concrete cubes, small beams and cylinders were casted from the concrete mix used in the specimens to examine the mechanical properties (compressive and tensile strengths) of the concrete. The average compressive strength obtained was about 35 MPa. The average measured tensile strength equal to 3.5 MPa. The mechanical properties of the two types of steel bars were investigated. Results are given in Figure 8.

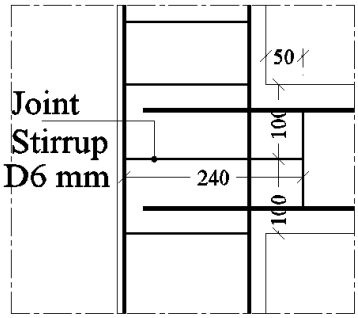

Figure 6. Reinforcement configurations (details of joint A) of the tested specimens Sp2

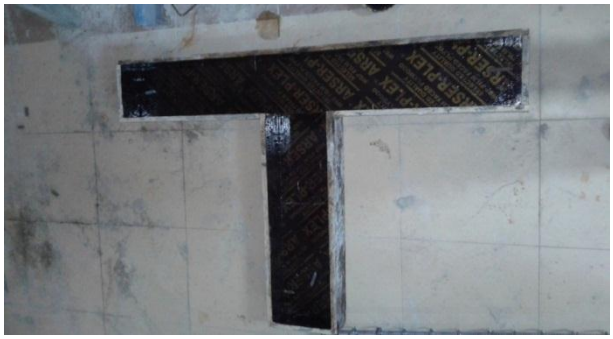

Figure 7. Form works that used for casting

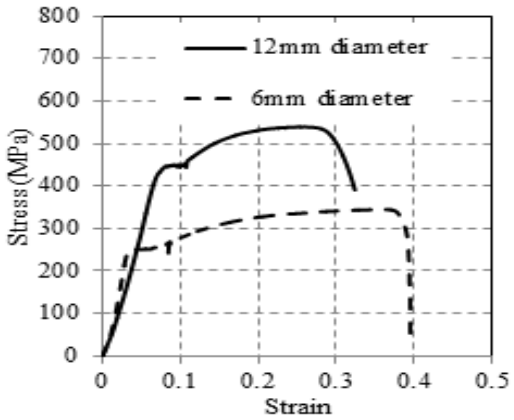

Figure 8 Stress and strain curves of rebars used

D. Testing Setup

The experimental work was performed on the testing rigid frame. Three manual hydraulic jacks were used in the test. The vertical and horizontal deflections were recorded using displacement gauges of sensitivity of 0.01mm. All readings were recorded manually. The experiment described in Figure 9 was utilized for research purposes.

E. Instrumentation

The vertical deflection at the free end of the beam (Δ1) was measured using a dial gauge with a maximum displacement of 50 mm. The horizontal movement of the column was measured by another displacement gauge (Δ2) at the top column's mid-point.

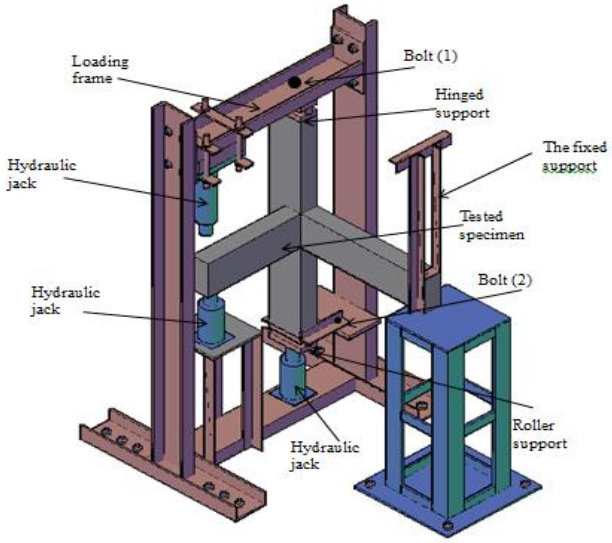

(a)

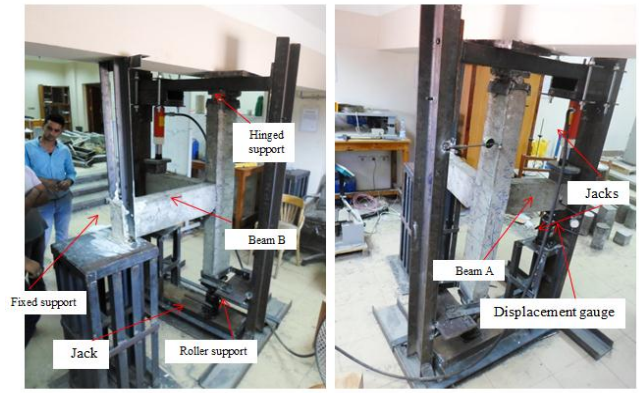

(b)

Figure 9. The test set-up

It was accurate to 0.01 mm. Figure 10 depicts the column's horizontal displacement (Δ2) and the beam's vertical deflection (Δ1). At each cycle of the test, the vertical beam tip deflection and crack development were observed. Figure 10 shows instrumentation of any specimen. Figure 11 and Figure 12 show details of instrumentation positions in different directions of loading.

F. Cyclic loading sequence

The load procedure proposed by [41] is employed in this investigation. The reversible cyclic loading was applied using two hydraulic jacks situated at the beam end. Figure 13 depicts the loading cycle history in the current investigation. The total number of cycles was fourteen. Each cycle was 2 mm bigger than the preceding one. The first cycle was split into two halves. For the first stage, the higher jack loaded the free end of the beam downward until the vertical displacement reached 2mm, at which point the upper jack's load was removed. The bottom jack was employed to keep the beam in its original position. The free end of the beam was loaded upward using the lower jack for the second step until the vertical displacement reached -2mm. The bottom jack's load was freed. The technique was repeated for the next cycle, but this time the displacement limit was increased by 2 mm from the previous one.

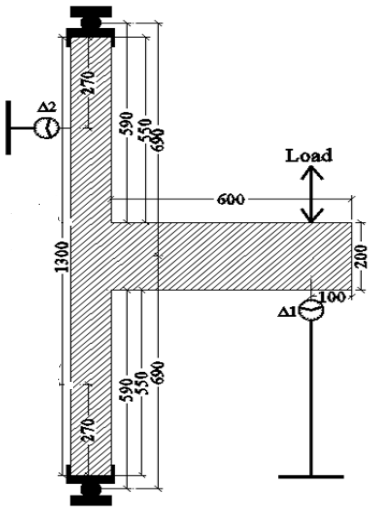

Figure 10 the displacement location of the tested specimens

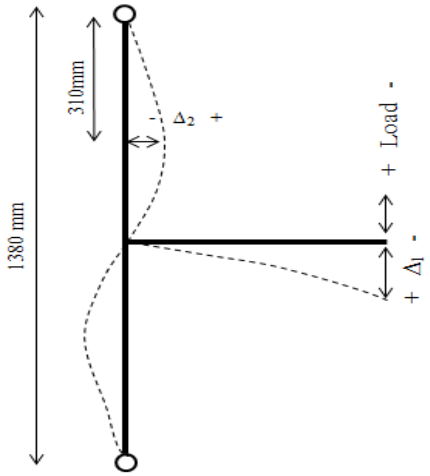

Figure 11. Instrumentation position details and projected distorted geometry (down loading).

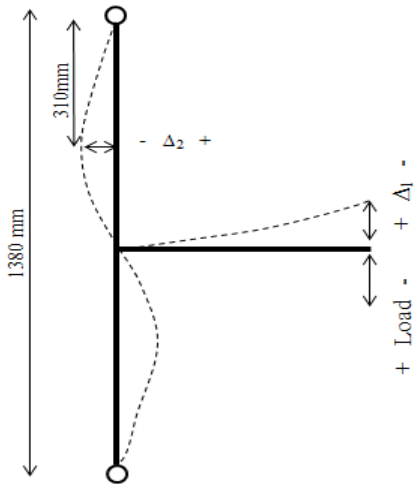

Figure 12. Instrumentation position details and projected distorted geometry (up loading)

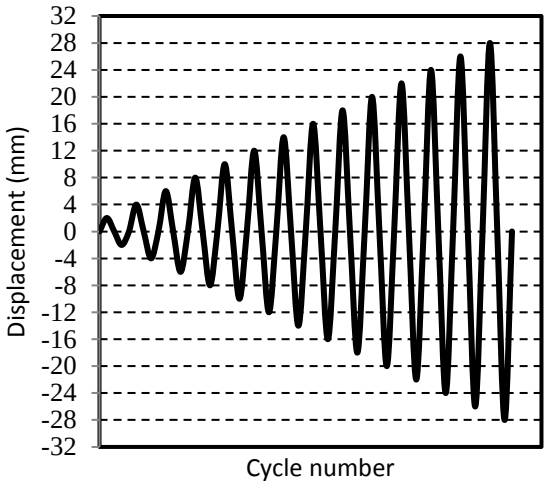

Figure 13. Cyclic loading histories

4. RESULTS

A. Ultimate and Cracks Loads

The eccentricity of the beam (A) from the column edge was 0, 25mm and 50 mm in Sp_0, Sp_1 and Sp_2, respectively. In addition, specimen Sp_2 had joint stirrup extended out the column core. Ultimate and crack loads of the tested BCCs are reported in Table 5. For all specimens, the first crack took placed at the loaded beam (A). For Sp_0, Sp_1, the first crack occurred in the first cycle at 9kN, 10 kN. As the shift of the beam increased, the unloaded beam (B) loaded by shear stresses more. For the 1st crack of the front face in joint for all specimens, it delayed about the 1st crack in the loaded beam (A). It was found that the 1st crack of the joint side delayed about the front and back face of the joint because of the eccentricity of the loaded beam was carried out faraway this side. Also direction of the loading was carried out perpendicular on the front and the back face of the joint in addition to center of transmitted load was applied faraway the right side of the joint.

For Sp_2, the 1st crack appeared at 11kN at three locations; the first is the joint from front, the second is the joint from the back and the last is the unloaded beam. Torsion cracks in the unloaded beam (B) were continued in the propagation. The first crack of the loaded beam (A) appeared at 13 kN.This means that the fixation degree was not affected by stirrup configuration. The 1st crack of unloaded beam of Sp_2 appeared at 11 kN. This mean that the 1st crack of unloaded beam of Sp_2 appeared faster than Sp_1 because of that the stirrup of Sp_2 make better connection between the column and the unloaded beam. Also, the crack of the joint of Sp_2occurred at higher loads than those corresponding to the cracks of the loaded and unloaded beams. This may be because of the fact that the eccentricity of the unloaded beam transmitted extra load to the unloaded beam instead of the joint.

The load carrying capacity of the specimen Sp_0, Sp_1 was 22.35 kNand 17 kN respectively, as illustrated in Table 5. Where P_{cr}= cracking load, P_u = ultimate load,and Δ_u = ultimate deflection at free end of the loaded beam (A).

As the shift of loaded beam (A) from the column increases, the load capacity of the connection decreases. This may be due to the fact that the unloaded beam attracts part of the stresses generated on the joint from the loaded beam. Also, it was noticed that the vertical displacement (Δ_u) of free end of the loaded beam at maximum load was affected by increasing the shifting.

The maximum load capacity of the specimen Sp_2 was 18.7kN. When the joint stirrup was extended out the column core, the capacity of the connection increased. Also, it was noticed that the ultimate displacement (Δ_u) of free end of the loaded beam (A) at maximum load was affected by increasing of the joint stirrup length.

Table 5. Test results of crack and ultimate loads

Specimen	P_{cr} (kN) Loaded beam	P_{cr} (kN) unloaded beam	P_{cr} (kN) Joint			P_u (kN) Maximum load	Δ_u(mm) at Maximum load
			Front face	side face	Back face		
Sp_0	9	20	12	17	17	22.35	20
Sp_1	10	14.5	11.6	12	11.6	17	20
Sp_2	13	11	11	17	11	18.7	16

B. Load Deflection Behavior

During the experiment, fourteen cycles were performed on reference specimen Sp0. The load-deflection graphs were obtained at every cycle. Figure 14 depicts the load-deflection curve of Sp0 for all 14 cycles to allow for self-comparison of one specimen. Each cycle was 2mm longer than the preceding one. The first cycle was split into two halves. For the first stage, the upper jack loaded the free end of the beam downward until the vertical displacement reached 2mm. the load of the higher jack was relieved. To restore the beam to its original position (deflection = 0.0 mm), the bottom jack was employed. The free end of the beam was loaded upward using the lower jack for the second step until the vertical displacement reached -2mm. The bottom jack's load was eliminated. The higher jack was used to restore the beam to its original horizontal position. The following cycles used the same approach.

The residual displacement in any cycle was found to be greater than the residual displacement in the preceding cycle. This could be due to cracks spreading with subsequent cycles. Any current cycle's curve slope was smaller than the previous cycle's curve slope. At the same level of loading, the rate of deflection increased as the cycle number increased. This might be due to the stiffness diminishing as the number of cycles increases. Another factor was the proliferation of fractures in any cycle greater than the preceding.

The deflection value during load release was greater than the deflection value during load rise at the same load level, according to all Sp0 curves for all cycles. This was owing to the specimen's poor stiffness after loading. The area encompassed by the load versus deflection charts was used to calculate the energy wasted in each cycle. The area within each cycle was computed in kN.mm and is shown in Table 6. It was

discovered that the energy wasted by the first cycle was close to zero.

The energy wasted by the cycle increased when the specimen was loaded with higher cyclic load. The column chart in Figure 15 depicted the rate of increase in energy dissipated for all Sp0 cycles. The increase in energy dissipated before to the commencement of the test was greater than the increase in area throughout the test. The energy expended began to decrease after the 12th cycle.

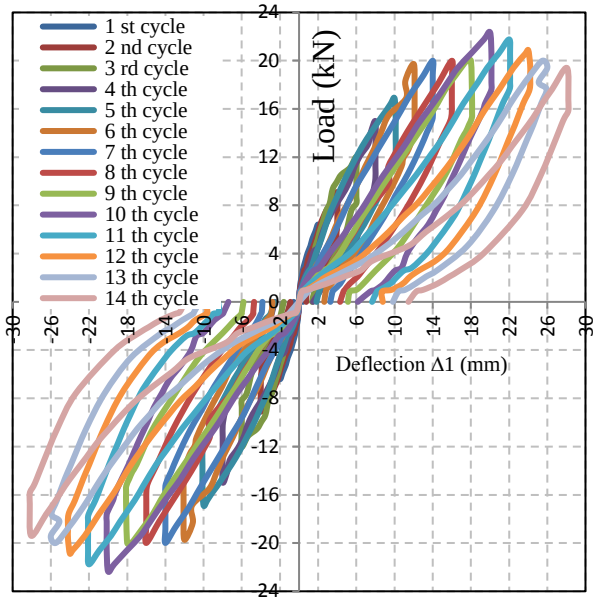

Figure 14 Load- deflection curve of Sp0-Δ1 for all cycles.

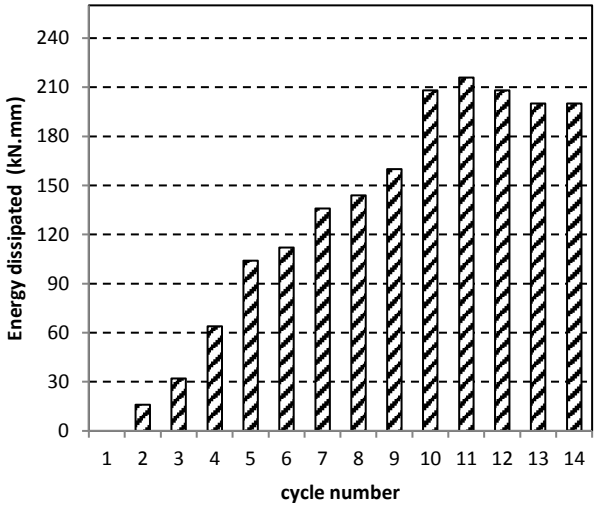

Figure 15. Rate of increase in the energy dissipated for each load–deflection curve of the specimen Sp0.

The experiment was carried out on shifted specimen Sp1 till failure after 11 rounds. During the test, the load-deflection curves were drawn at each cycle. Figure 16 depicts the load-deflection curve of Sp1 for all cycles in order to do a self-comparison of one specimen. The residual deflection at any cycle was greater than the residual deflection at the preceding cycle, based on the behaviour of the specimen in deflection. This might be due to fractures spreading with subsequent cycles. Any current cycle's curve slope was smaller than the previous cycle's curve slope. This signifies that the deflection rate has risen. The deflection value during load release was greater than the deflection value during load rise at the same load level, according to all Sp1 curves for all cycles. The same deflection behaviour was seen in comparative sample Sp0.

The area encompassed by the load versus deflection charts was used to calculate the energy wasted in each cycle. Table 7 shows the area inside each curve computed in kN.mm. It was discovered that the energy wasted during the first cycle was approximately 8 kN.mm. During the loading, the energy dissipated increased. The column chart in Figure 17 depicted the rate of increase in energy dissipation for all Sp1 cycles. The energy wasted rose progressively until the eighth cycle, then it remained constant for the eighth, ninth, and tenth cycles. The energy expended began to decrease after the 11th cycle.

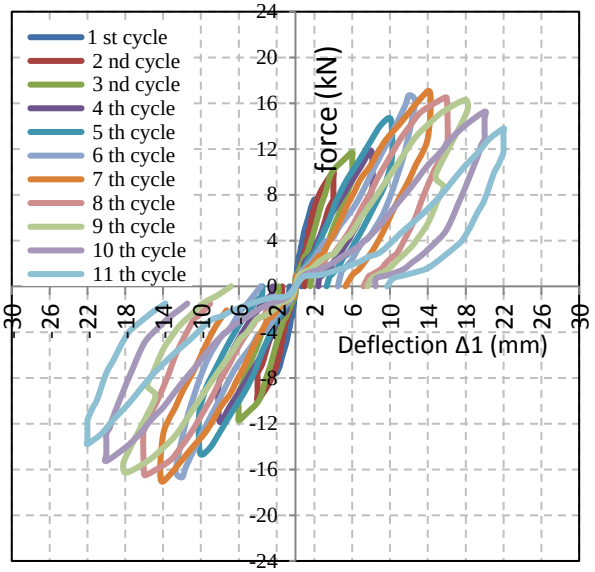

Figure 16. Load- deflection curve of Sp1 -Δ1 for all cycles.

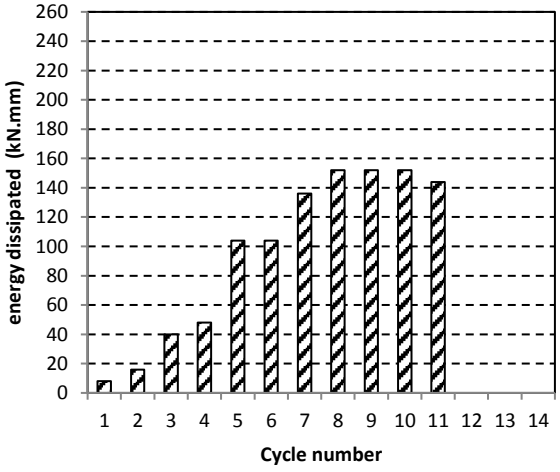

Figure 17. Rate of increase in the energy dissipated for each load–deflection curve of the specimen Sp1.

During the experiment, 14 cycles were performed on specimen Sp2 till failure. Figure 18 depicted the load-

deflection curves for Sp2 at each cycle. When comparing two successive cycles, the slope of the curve dropped as the loading increased. Furthermore, the load at the cycle end rose until the 10th cycle, after which it decreased. The area encompassed by the load versus deflection charts was used to calculate the energy wasted in each cycle. The energy wasted for each cycle curve was calculated in kN.mm and is shown in Table 8.The first cycle wasted roughly 0 energy. The energy dissipated increased when the specimen was subjected to increasing cyclic stress. The column chart in Figure 19 depicted the rate of increase in energy dissipation for all Sp2 cycles. At the 10th cycle of the specimen Sp2, the area reached its maximum value. The energy dissipated rise showed a consistent gradient in the first eight cycles. The growth began abruptly in the ninth cycle and continued until the tenth cycle. The region shrank after the tenth cycle.

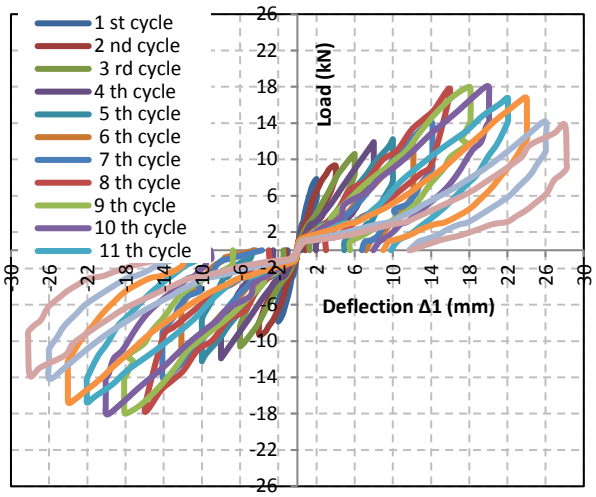

Figure 18. Load-deflection curve of Sp2-Δ1 for all cycles.

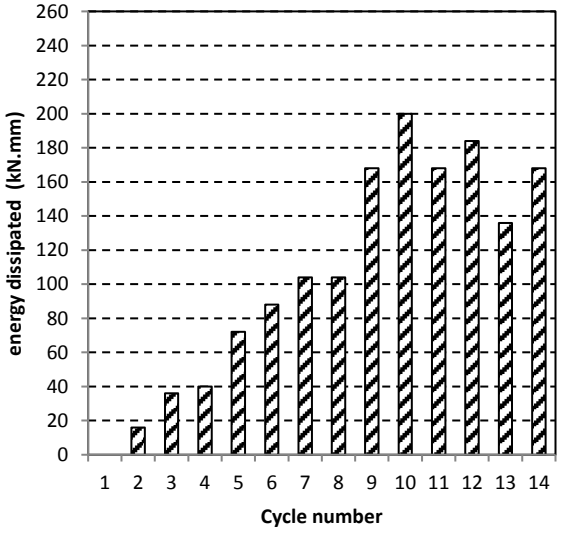

Figure 19. Rate of increase in the energy dissipated for each load–deflection curve of the specimen Sp2

The relationship between the load at the cycle end and the corresponding deflection for all specimens is plotted in Figure 20. The curve has the same number of points as the number of cycles. Each point represented the cycle's apex (displacement mm, load kN).The peaks curve for Sp_0, Sp_1 and Sp_2 was induced. All specimens had same trend. The load versus the deflection curve has a nonlinear relationship. The rate of variation was non uniform. At a specific displacement, the peak of Sp_0 was the largest while the capacity of Sp_1 was the smallest. Also, at the same level of the load, the deflection of Sp_1 was the biggest while the deflection of Sp_0 was the smallest. This may be due to the shifting 25 mm of Sp_1. Although, the shift increased into 50 mm in Sp_2, the deflection response improved due to the stirrups extended outside the column core.

5. CONCLUSION AND FUTURE RESEARCH

In this work, an experimental study that consisted of three RC eccentric beam column joint (1/3 scale model) was induced. The specimens were examined under reversible cyclic loading. The effect of shifting of the beam outside the column and the stirrups configuration were studied. The test results showed the following remarks:

- The failure of the specimen had loaded beam (A) without shifted outside the column edge occurred at the connection between the loaded beam (A) and the column.
- The failure of the specimens that shifted outside the column edge was occurred at the connection between the unloaded beam (B) and the column.
- It was noticed that when the loaded beam (A) have main bars extended outside the column core, the capacity of the connection decreased.
- The ultimate load of specimen Sp_1, which was shifted by 25mm, was less than the ultimate load of specimen Sp_0, without shift, by 24%.
- The failure was occurred at the unloaded beam (B) beside the connection when the joint was reinforced by a stirrup extended out the column core.

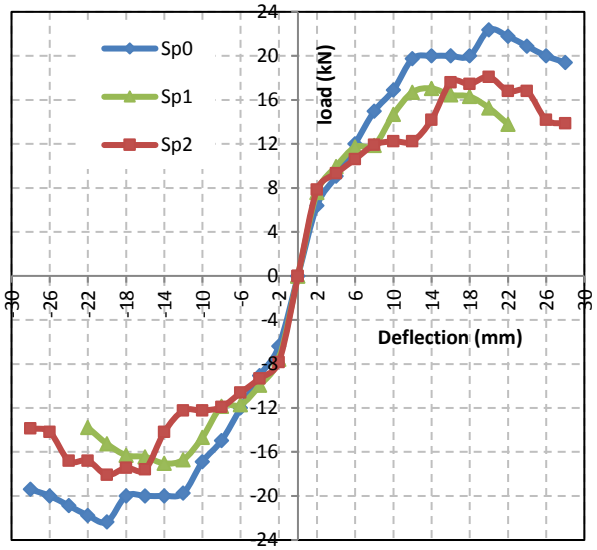

Figure 20. Envelope relationships of the BCCs

Table 6. Energy dissipated for each load–deflection curve of the specimen Sp0

Cycle number	The 1st	The 2nd	The 3rd	The 4th	The 5th	The 6th	The 7th	The 8th	The 9th	The 10th	The 11th	The 12th	The 13th	The 14th
Area (kN.mm)	0	16	32	64	104	112	136	144	160	208	216	208	200	200

Table 7. Energy dissipated for each load – deflection curve of the specimen Sp1.

Cycle number	The 1st	The 2nd	The 3rd	The 4th	The 5th	The 6th	The 7th	The 8th	The 9th	The 10th	The 11th	The 12th	The 13th	The 14th
Area (kN.mm)	8	16	40	48	104	104	136	152	152	152	144	--	--	--

Table 8. Energy dissipated for each load–deflection curve of the specimen Sp2.

Cycle number	The 1st	The 2nd	The 3rd	The 4th	The 5th	The 6th	The 7th	The 8th	The 9th	The 10th	The 11th	The 12th	The 13th	The 14th
Area (kN.mm)	0	16	36	40	72	88	104	104	168	200	168	184	136	168

- When the joint stirrup was extended outside the column core by 50 mm in specimen Sp_2, the capacity of the connection increased.
- It was showed that the increase of stirrup length in the joint decreased the deflection at the same level of the load.

The following suggestions may be recommended for investigation in the future:-

- The effect of the column width on behavior of the RC beams column connection under static loads.
- The effect of the column width on behavior of the RC beams column connection under seismic loads.
- The effect of the concrete compressive strength on behavior of the RC beams column connection under seismic loads.
- The effect of presence of the slab on behavior of the RC beams column connection under seismic loads.
- Study of structural performance of the RC beams column connection under different cyclic loading histories.
- Experimental investigation of effect axial column load on structural performance of the RC beams column connection under cyclic loads.
- Experimental investigation of effect axial beam load on structural performance of the RC beams column connection under cyclic loads

Acknowledgements
The current work is an outgrowth of the first author's Doctor of Philosophy thesis. The tests were carried out in the RC Laboratory, Faculty of Engineering, Kafrelshiekh University, Egypt.

Funding: This research has not received any type of funding.

Conflicts of Interest: The authors declare that there is no conflict of interest.

REFERENCES

[1] Yasuaki GOTO, Osamu JOH "shear resistance of RC interior eccentric beam-column joints" 13th World Conference on Earthquake Engineering Vancouver, B.C., Canada August 1-6, 2004, Paper No. 649.
[2] Akanshu Sharma , G.R. Reddy, R. Eligehausenb, K.K. Vaze "Strength and ductility of RC beam-column joints of non-safety related structures and recommendations by national standards" journal of Nuclear Engineering and Design , volume 241 pp.1360–1370, 2011.
[3] Hideo Murakami, shigerufujii, yasuhiroishiwata and shiromorita "shear strength and deformation capacity of interior R/C Beam-column joint sub assemblage" conference of 12 WCEE, 2000.
[4] Sangjoon Park, Khalid M. Mosalam "Parameters for shear strength prediction of exterior beam–column joints without transverse reinforcement" Engineering Structures 36 (2012) 198–209.
[5] Jung-Yoon Lee , Jin-Young Kima, Gi-Jong Oh "Strength deterioration of reinforced concrete beam_column joints subjected to cyclic loading" Engineering Structures 31 (2009) 2070_2085.
[6] F. Kusuhara1 and H. Shiohara "Tests of R/C Beam-Column Joint with Variant Boundary Conditions and Irregular Details on Anchorage of Beam Bars" The 14th World Conference on Earthquake Engineering October 12-17, 2008, Beijing, China.
[7] Leslie M. MEGGET1, Meg B. BARTON, and Richard C. FENWICK "seismic design and behavior of external reinforced concrete beam-column joints using 500E grade steel reinforcing" 13th World Conference on Earthquake Engineering Vancouver, B.C., Canada August 1-6, 2004 Paper No. 3472.
[8] MinakshiVaghani , Dr. S.A. Vasanwala , Dr. A.K. Desai, "Performance of RC Beam Column Connections Subjected to Cyclic Loading " IOSR Journal of Mechanical and Civil Engineering, Volume 12, Issue 2 Ver. VII (Mar-Apr 2015): 48-53. doi:10.9790/1684-12274853.
[9] Benavent-Climent, A., X. Cahís, and R. Zahran. "Exterior Wide Beam–column Connections in Existing RC Frames Subjected to Lateral Earthquake Loads." Engineering Structures 31, no. 7 (July 2009): 1414–1424. doi:10.1016/j.engstruct.2009.02.008.
[10] Elsouri, A.M., and M.H. Harajli. "Seismic Response of Exterior RC Wide Beam–narrow Column Joints: Earthquake-Resistant Versus as-Built Joints." Engineering Structures 57 (December 2013): 394–405. doi:10.1016/j.engstruct.2013.09.032.
[11] Bohara, Rajendra Prasad, GanchaiTanapornraweekit, and SomnukTangtermsirikul. "Experimental and numerical investigation on seismic performance of a composite wide beam-column interior joint." Structures.Vol. 30. Elsevier, 2021.
[12] Wang, Ying, et al. "Experimental and numerical investigation on progressive collapse resistance of RC frame structures considering transverse beam and slab effects." Journal of Building Engineering 47 (2022): 103908.
[13] Shen, Xinyu, et al. "Experimental and numerical study on reinforced concrete beam-column joints with diagonal bars: Effects of bonding condition and diameter." Structures.Vol. 37. Elsevier, 2022.
[14] Zhang, Chao, et al. "Experimental and numerical investigation on seismic performance of retrofitted RC frame with sector lead viscoelastic damper." Journal of Building Engineering 44 (2021): 103218.
[15] Rong, Bin, et al. "Experimental and numerical investigation on seismic performance of S-RC-SRC composite joint." Journal of Building Engineering 43 (2021): 103079.
[16] Baciu, Catalin, et al. "Experimental and numerical studies of the progressive collapse of a reinforced concrete-framed structure using capacity curves." Arabian Journal for Science and Engineering 44.10 (2019): 8805-8818.

[17] Fayaz, Qurrain, GurbirKaur, and Prem Pal Bansal. "Numerical Modelling of Seismic Behaviour of an Exterior RC Beam Column Joint Strengthened with UHPFRC and CFRP." Arabian Journal for Science and Engineering 47.4 (2022): 4971-4986.
[18] Fayed, Sabry, Walid Mansour, and Magda H. Farhan. "Using Surveying Instruments in Monitoring 3D Deformations of RC Structure Subjected to Differential Settlement of Its Footings." Arabian Journal for Science and Engineering (2022): 1-22.
[19] Ahmed Elezaby, Mohammed Zayed, Sabry Fayed, Mohammed Elzeir, Ali Basha "experimental verification of gradually varied flow profile computation" Conference Paper · September 2009. DOI: 10.13140/RG.2.1.3129.3928.
[20] A.Khalil, E.Etman, A.Atta, and S.Fayed "Strengthening of RC Box Beams Using External Prestressing Technique" the 10th International Conference on The "Role of Engineering Towards a Better Environment" (RETBE'14), 15-17 December, 2014 at HelnanPalastine Hotel in Alexandria.
[21] Abd El-Hakim Khalil, EmadEtman, Ahmed Atta, Sabry Fayed "Torsional Strengthening of RC Box Beams Using External Prestressing Technique" IOSR Journal of Mechanical and Civil Engineering, Volume 12, Issue 2 Ver. VII (Mar - Apr. 2015), PP 30-41.www.iosrjournals.org.
[22] Ahmed G. Asran1, Hassan H. EL-Esnawi, Sabry Fayed "Numerical Investigation of RC Exterior Beam Colum Connections under Monotonic Loads" IOSR Journal of Mechanical and Civil Engineering (IOSR-JMCE), Volume 13, Issue 1 Ver. VI (Jan- Feb. 2016), PP 60-67. www.iosrjournals.org
[23] Ahmed G. Asran, Hassan H. EL-Esnawi, Sabry Fayed "A Review on Reinforced Concrete Beam-Column connections" 11th international conference on civil and architecture engineering ICCAE-11, April 19-21, 2016, Cairo, Egypt.
[24] Ahmed G. Asran, Hassan H. EL-Esnawi, Sabry Fayed "Behavior of RC beam-column joint under cyclic loads" the ninth alexandria international conference on structural and geotechnical engineering (AICSGE9), 19 – 21 December 2016.
[25] Ahmed G. Asran, Hassan H. EL-Esnawi, Sabry Fayed "Experimental Investigation of RC Exterior Beam Column Connection with Eccentric Beam Subjected to Reversible Quasi Static Loads" Civil Engineering Journal Vol. 3, No. 4, April, 2017, PP:221-236.
[26] A. M. Basha a*, Sabry Fayed "Behavior of RC Eccentric Corner Beam-Column Joint under Cyclic Loading: An Experimental Work" Civil Engineering Journal, Vol. 5, No. 2, February, 2019, PP: 295-308.
[27] Ali Basha, Sabry Fayed, and GalalElsamak "Flexural Behavior of Cracked RC Beams Retrofitted with Strain Hardening Cementitious Composites" KSCE Journal of Civil Engineering, April 9, 2019, PP:1-13. DOI 10.1007/s12205-019-1874-4
[28] Sabry Fayed, Ali Basha, Ahmed Hamoda "Shear strengthening of RC beams using aluminum plates: An experimental work" Construction and Building Materials 221 (2019) 122–138.
[29] Hamoda, A., Basha, A., Fayed, S., &Sennah, K. (2019). Experimental and Numerical Assessment of Reinforced Concrete Beams with Disturbed Depth. International Journal of Concrete Structures and Materials, 13(1), 55.
[30] Fayed, S. (2019). Flexural Strengthening of Defected RC Slabs Using Strain-Hardening Cementitious Composites (SHCC): An Experimental Work. Arabian Journal for Science and Engineering, 1-12.
[31] Elsamak, G., & Fayed, S. (2020). Parametric studies on punching shear behavior of RC flat slabs without shear reinforcement. Computers and Concrete, 25(4), 355-367.
[32] Basha, A., Fayed, S., & Mansour, W. (2020). Flexural strengthening of RC one way solid slab with Strain Hardening Cementitious Composites (SHCC). Advances in concrete construction, 9(5), 511-527.
[33] Fayed, S., Basha, A., &Elsamak, G. (2020). Behavior of RC stepped beams with different configurations: An experimental and numerical study. Structural Concrete.
[34] Fayed, S., & Mansour, W. (2020). Evaluate the effect of steel, polypropylene and recycled plastic fibers on concrete properties. Advances in concrete construction, 10(4), 319-332.
[35] Mansour, W. & Fayed, S. (2021).Effect of interfacial surface preparation technique on bond characteristics of both NSC-UHPFRC and NSC-NSC composites. Structures, 29, 147–166.
[36] ElsamakGalal, and Sabry Fayed. "Flexural strengthening of RC beams using externally bonded aluminum plates: an experimental and numerical study." Advances in concrete construction 11.6 (2021): 481-492.
[37] Baraghith, Ahmed T., et al. "Effectiveness of SHCC strips reinforced with glass fiber textile mesh layers for shear strengthening of RC beams: Experimental and numerical assessments." Construction and Building Materials 327 (2022): 127036.
[38] ACI Committee 318 (2018) Building Code Requirements for Structural Concrete (ACI 318-18). American Concrete Institute.
[39] Kiran, R., and Genesio, G., (2014), "A case study on pre 1970s constructed concrete exterior beam-column joints", Case Studies in Structural Engineering, Vol.1, pp. 20–25.
[40] Egyptian Code for Design and Construction of Reinforced Concrete Structures, (ECP 203-2007) 2007.
[41] Kularni, S. M., and Patil, Y. D., (2013), "A Novel Reinforcement Pattern for Exterior Reinforced Concrete Beam-Column Joint", Procedia Engineering, Vol. 51, pp. 184 – 193.